Research article

Biomarker characteristics of Montney source rock, British Columbia, Canada

Azzam Barham [*], Mohd Suhaili Ismail, Maman Hermana, N.S. Zainal Abidin

Geosciences Department Universiti Teknologi Petronas, Perak, Malaysia

HIGHLIGHTS

- Geochemical analyses of biomarker traces, elemental analysis, and pyrolysis provide a continuous profile of source rock.
- The OM source input, preservation conditions, and thermal maturation level were provided based on biomarker analysis.
- The results of the elemental analysis show that the Montney formation source rock was deposited in a marine environment.
- Biomarkers are considered an effective method for detailed and insightful information that helps evaluate any source rock.

ABSTRACT

Montney Formation (MF) source rock located in northeastern British Columbia (BC), Canada, was analyzed to determine its depositional conditions and organic matter source input other than to determine their level of thermal maturity. The high total sulfur (TS) (2.23–20.86 wt.%) and good to very good total organic carbon (TOC) content (0.3–5.87 wt.%) in the analyzed samples give good evidence that the deposition of MF source rock was in a marine environment under reducing conditions. A mixed marine-terrestrial derived organic matter (OM) for the Montney source rock that was deposited in a marine dysoxic environment is deduced from the composition and distribution of different biomarker traces. Thus, the previous result is supported by the high short-chain n-alkanes ratio, accompanied by carbon preference index (CPI) around unity, high concentration of tricyclic terpanes, high C_{24} tricyclic/C_{24} tetracyclic, hopane/sterane ratios ranging from low to moderate, as well as the relationship between regular sterane compositions. During deposition of the MF source rock, it can be noticed that more land organic materials this was deduced according to the high waxiness index. From maturity ratios of Ts/(Ts + Tm), C_{32} 22S/(22S + 22R) homohopane, moretane/hopane and 20S/(20S + 20R) and $\beta\beta/(\beta\beta + \alpha\alpha)$ C_{29} it can give a conclusion that the source rock is mature to postmature of hydrocarbon generation.

1. Introduction

The Lower Triassic Montney Formation (MF) of the Western Canada Sedimentary Basin (WCSB) (Figure 1) is a world-class unconventional resource with 450 Tcf gas reserves, 14 520 million barrels of marketable natural gas liquids reserves, and 1125 million barrels of commercial oil reserves [1]. Although commonly described as shale, the MF is siltstone in most of its subcrop. MF is a multilayered accumulation of fine-grained sediments (shale, siltstone, sandstone) deposited in the offshore to shoreface environment [2].

Unconventional reservoirs have been studied intensively in the last two decades because they form cap rocks and are an essential and direct source of hydrocarbons, especially after the production of conventional storage tanks began to decline and the inability to cover the growing market needs. But these reservoirs need recent and in-depth studies using different techniques to create models as a reference for proper understanding and determining reservoir parameters.

Classification of source rocks and labeling the families of the crude oils became possible and easy to achieve by using petroleum geochemistry [3, 4, 5, 6, 7, 8, 9, 10]. Organic matter (OM) extract analysis is one of the most basic tests for determining paleo-preservation conditions, OM maturity, and the type of hydrocarbons generated [11, 12]. These parameters will help in locating hydrocarbons in the basin's explored areas and various stratigraphic units [13]. This kind of analysis is also beneficial in developing tools describing, understanding, and predicting the formation of sweet spots of oil and gas, migration, basins thermal maturity history, and fluids that have passed through them all over exploration and production. The OM extract analyses include
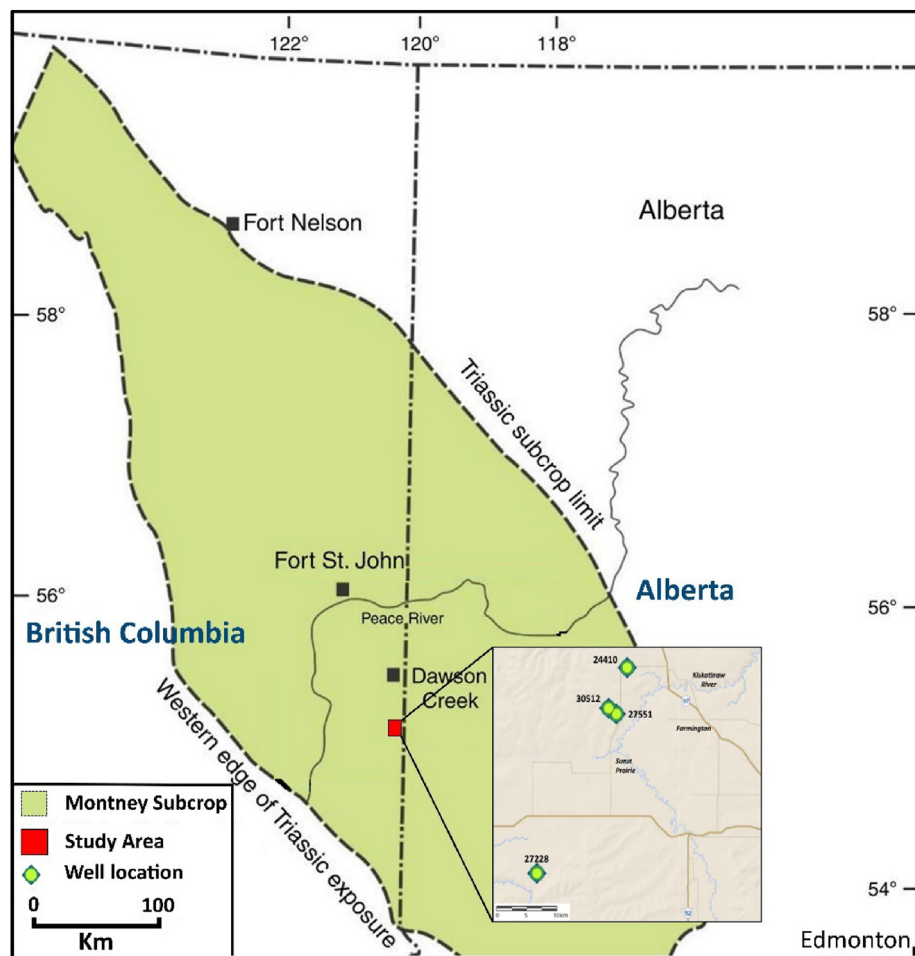
Figure 1. Location map of the studied wells, Montney subcrop, northeastern BC, Canada.

biomarkers, stable isotope ratios, hydrocarbon contents [8]. The biomarkers analysis using gas chromatography-mass spectrometry (GC-MS) is the key to this information. As a result, petroleum geochemistry has become a widely used tool in the oil and gas industry [14].

Source rock potential and OM maturity of the MF were the focus of most of the studies; very few organic geochemical investigations on the origin of OM and the preservation conditions during deposition have been made. Biomarkers were not heavily used in assessing the MF source rock because most previous interpretations relied heavily on pyrolysis methods, which indicated the largely gas-prone nature of the probable source rock in the MF without thoroughly investigating the source input and preservation conditions of the OM. Riediger [15] first made correlations for the oil-source rock of the Triassic source rocks in BC, which were established, based on biomarker traces; the results of the study revealed that the over mature stage of MF nearly in most of the studied area, which makes it difficult to assess its (original) source potential. The current study aims to provide a detailed overview of the OM source input, preservation conditions, and thermal maturation level of the MF source rock depending on a detailed biomarkers analysis.

2. Geological setting

The lower Triassic Montney sediments deposited in a basin presently known as the WCSB on the Pangean supercontinent west margin, The Peace River's central basin is considered one of the essential sub-basins inside the WCSB [16, 17, 18, 19, 20]. The MF reaches up to 300 m of deltaic marine and submarine turbidites deposited in the peace river arc area of NE BC. The lower Triassic MF was assigned to the Griesbachian to Spathian in age [19] (Figure 2). In nearly most places, the Triassic sequence overlies unconformably overlies the Carboniferous to Permian (Belloy Formation) strata [15, 21, 22, 23]. The Triassic sequence's cumulative thickness is approximately 1200 m in the westernmost outcrop in the Rocky Mountain bottoms [21]. The main sediment types include deeper water, interlaminated shale with siltstone, and fine-grained sandstone, which reveal a turbidity condition [21, 24, 25] (Figure 2). The stratigraphy and the paleogeography of the MF were established based on the Induan and Lower Olenekian aged deposits that contain the shallow marines and turbiditic facies [24, 26, 27]. The various sedimentary environments are presented, including Tidal and wave-dominated foreshore, shoreface, and offshore settings, forming the typical facies association and log pattern [27] (Figure 2).

The early Triassic was a time of biologic recovery as it immediately follows the End-Permian extinction, the most severe biologic perturbation in history [2, 29, 30]. Regionally extensive shallow water anoxia/dysoxia in conjunction with increased oceanic acidity is thought to have played a significant role in the extinction [31, 32, 33]. These conditions are assumed to have continued into the Early MF [32, 33]. On the basis of lithology, mineralogy, and well log character, the MF is formally divided into eight regionally extensive members. The major three are the Lower Montney Member, the Middle Montney Member, and the Upper Montney Member, which correspond to the informal units used by
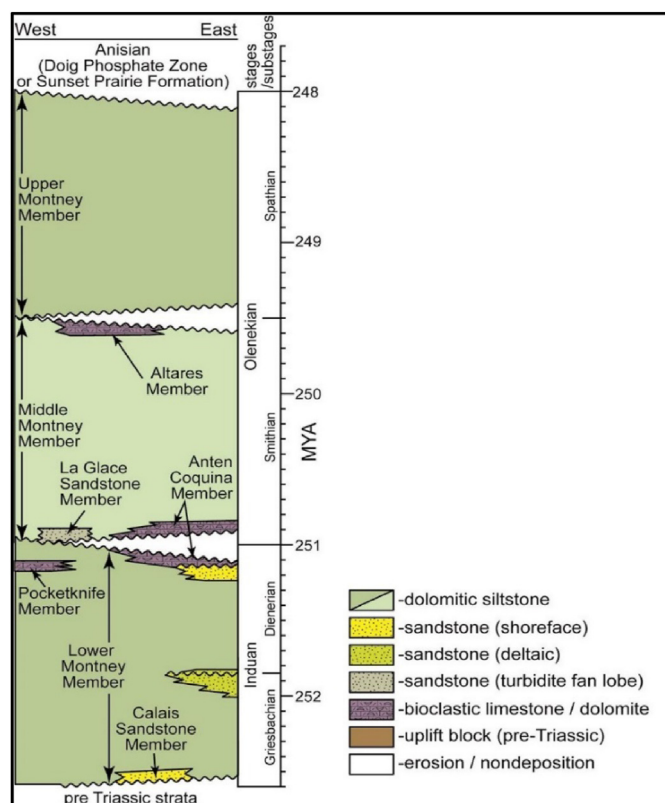
Figure 2. Ideal stratigraphic sequence of the MF [28].

industry geoscientists. The boundaries of these units correspond to those of main boundaries (Dienerian-Smithian and Smithian-Spathian) [24, 34, 35, 36].

3. Samples and methods

Thirty-four core samples were collected from four wells in the BC area (Figure 1). These wells were chosen to cross distinct lithofacies in a northeast-southwest direction. Before the geochemical studies, the collected samples were thoroughly cleaned. Geochemical analyses of the obtained samples were carried out at the Universiti Teknologi PETRO-NAS (UTP) and STRATOCHEM Laboratories, respectively. The samples were crushed to powder and separated into three parts; a small amount (1.5–2 mg) of the dry sample was used for elemental analysis using a PerkinElmer 2400 Elemental Analyzer (CHNO/S), which can provide measurements of the sulfur contents (TS) for preservation conditions. The second section was utilized for pyrolysis analysis and total organic carbon (TOC) measurement, with the SRA (source rock analyzer) employed to determine source rock potentiality and maturity. Pyrolysis analysis entails heating to 650 °C in an inert environment and measuring parameters such as S_1, S_2, and Tmax (Table 1). Following that, the hydrogen index (HI), production index (PI), and potential petroleum yield (PY) were computed (Table 1). Because of the possibility of interferences between some classes of aromatic and saturate biomarkers, it is customary to separate saturates and aromatics components by liquid chromatography (MPLC, for example) before the examination so that each fraction may be studied separately. Both saturate and aromatic fractions were examined using an HP 6890 gas chromatograph outfitted with an HP 7683 auto-sampler, on-column injector, and the HP5973 mass selective detector (MSD); the sample preparation and investigation followed the procedure suggested by [37, 38, 39], and the results were used to determine the source of the organic material, maturity, and preservation conditions.

4. Results and discussion

4.1. Organic-carbon and sulfur contents

Table 1 shows that the MF source rock samples have relatively good to very good TOC as 80% of the results fall in the range of 1–4%. The good enrichment of OM in terms of TOC results indicates that the OM preservation conditions were low to moderate when the source rock's sediments were being deposited or could be due to exhausting OM [40, 41, 42].

The TS wt.% of studied source rock samples from MF was high and ranged between 2.23 and 21.97 wt.% (Table 1). There is no apparent correlation between TOC and TS, as shown in (Figure 3); this indicates no relation between TS and OM sedimentation in the tested source rock samples. The origin and condition of preservation of OM in the marine environment were determined by the cross plot between TOC and TS contents as shown in (Figure 3) [43, 44], elucidated that the use of TS as an indicator of marine effect is stronger than the organic or pyritic sulfur in the sediments. The highly reducing hypersaline marine conditions were marked by TS > 2 wt.% [45], whereas the non-marine (freshwater) sediments have concentrations of TS < 0.5 wt.% [43, 46]. Thus, regarding the MF source rock understudy samples, which contain high TS > 2 wt.%, the interpreted depositional environment is marine under highly hypersaline-reducing conditions (Figure 3).

4.2. Type and characteristics of organic matter

The pyrolysis results of the analyzed samples (Table 1) were the reference for evaluating OM richness, type of kerogen, and maturity. The pyrolysis S_1 and S_2 results were 0.52–8.44 mg HC/g rock and 0.42–2.89 mg HC/g rock, respectively (Table 1), showing high S_1 values regarding the S_2 be explained by the high contamination or recent migration of hydrocarbons [47]. However, S_2 values indicated that the generative potential of the MF source rock samples had fair to good (Figure 4), with comparatively low values of less than 2.89 mg HC/g rock (Table 1). The calculated HI and the low pyrolysis S_1 and S_2 yields were used to characterize the kerogen type. The low HI values, in the range of 33.02–209.45 mg HC/g TOC (Table 1) for the studied samples, places them in the kerogen type IV. A relationship was established using a pseudo van Krevelen graph of HI versus Tmax to infer the kerogen type and maturity level (Figure 5), which was assigned to kerogen type IV, indicating a thermally mature to postmature OM [48].

4.3. Biomarkers

Biomarkers, considered geochemical fossils, are defined as complex organic compounds composed of carbon found in crude oils, bitumen, and petroleum source rocks because they can be used as indicators of depositional environments in the same way we use the physical remains of organisms [50, 51]. Also, they can be related to the original biochemical precursor even after undergoing accumulation, diagenesis, and catagenesis [50].

Total ion current (TIC) and single ion monitoring (SIM) modes were used to record the normal alkanes, isoprenoids, terpenes, and steranes distributions. The TIC and SIM mode mass chromatograms (m/z 85, m/z 191, and m/z 217) were used as a reference for the detailed biomarker characteristics investigated in this study. And their identification was based on retention time and previous work [9, 10, 52]. The concentration ratios of the biomarkers were used as indicators of source input of the OM and the paleoenvironmental conditions during deposition of the MF source rock [3, 4].

Gas chromatograms of saturate fractions from four representative samples are shown in (Figure 6). The distribution of n-alkanes was used to indicate the source input of the parent organic organisms [53]. For example, the short-chain n-alkanes < C_{20} means algal-sourced OM, while

Table 1. TOC and main pyrolysis data results with calculated source rock parameters of the MF core samples.

Well ID	Max. depth (m)	Depth (m)	TS (wt.%)	TOC (wt.%)	S1 (mg/g)	S2 (mg/g)	Tmax (°C)	HI (mg/g)	OI (mg/g)	PI (mg/g)	PY (mg/g)
15-34-080-18W6	2062	2048.65	11.80	1.07	2.25	0.63	461	58.88	2.80	0.78	2.88
		2054.93	11.50	1.20	1.85	0.82	466	68.33	3.33	0.69	2.67
		2060.02	9.40	1.12	1.61	0.84	455	75.00	0.00	0.66	2.45
		1852.80	16.98	2.30	2.68	1.03	475	44.80	19.57	0.72	3.71
		1859.14	18.11	0.60	1.16	0.43	451	76.51	80.07	0.73	1.59
		1866.76	15.96	3.11	4.49	1.84	489	59.18	16.73	0.71	6.33
		1867.13	20.86	3.01	6.39	1.82	480	60.53	14.63	0.78	8.21
		1871.10	20.20	3.12	6.24	1.89	478	60.64	14.12	0.77	8.13
b-093-I/094-B-09	2061	1883.01	10.56	1.50	3.50	0.86	454	56.17	36.58	0.80	4.36
		1898.61	18.17	1.70	3.48	0.98	457	57.92	30.14	0.78	4.46
		1933.04	20.67	1.60	2.25	0.58	444	35.28	27.98	0.80	2.83
		1948.10	19.81	1.80	2.18	0.76	448	42.25	28.90	0.74	2.94
		1973.10	21.97	1.00	2.01	0.51	447	51.93	57.03	0.80	2.52
		1983.10	20.67	1.40	2.68	0.67	445	47.02	38.60	0.80	3.35
		1999.50	20.13	1.50	2.88	0.79	457	52.74	20.03	0.78	3.67
		2142.10	20.27	1.60	2.45	1.53	317	98.46	23.17	0.62	3.98
		2148.60	20.12	4.40	6.24	2.30	351	51.91	11.06	0.73	8.54
		2152.00	19.28	3.60	1.04	1.46	489	40.95	11.50	0.42	2.50
		2159.80	20.55	4.80	5.09	2.89	485	59.91	10.99	0.64	7.98
11-25-77-20W6	2834.5	2161.80	20.48	5.87	1.59	2.33	496	39.69	10.39	0.41	3.92
		2163.80	20.31	0.90	8.44	1.95	324	209.45	46.19	0.81	10.39
		2166.60	14.62	5.10	1.76	2.00	502	39.43	7.29	0.47	3.76
		2168.80	15.46	0.67	2.94	0.56	370	84.21	64.66	0.84	3.50
		2186.60	17.23	1.55	5.91	0.70	311	45.22	31.65	0.89	6.61
		2385.04	5.53	0.92	0.52	0.50	459	54.53	34.90	0.51	1.02
		2392.87	7.81	1.27	0.55	0.42	458	33.02	29.87	0.57	0.97
		2402.17	2.23	0.30	0.57	0.43	457	133.54	114.91	0.57	1.00
		2411.48	5.04	1.37	0.58	0.64	459	46.78	24.85	0.48	1.22
A01-17-080-18W6	2592.35	2420.67	4.47	2.36	0.88	1.07	474	45.30	17.36	0.45	1.95
		2429.81	5.77	2.10	0.94	1.26	486	60.75	16.39	0.43	2.20
		2438.76	5.41	1.90	0.98	1.02	477	52.50	17.50	0.49	2.00
		2447.88	4.82	1.93	1.04	1.11	477	57.51	17.10	0.48	2.15
		2457.33	4.75	3.00	1.65	1.56	486	51.97	11.33	0.51	3.21
		2465.14	3.31	1.42	0.96	0.51	471	35.97	21.16	0.65	1.47

TOC: Total organic carbon, wt.%.
S1: Volatile hydrocarbon (HC) content, mg HC/g rock.
S2: Remaining HC generative potential, mg HC/g rock.
HI: Hydrogen Index = S2 *100/TOC, mg HC/g TOC.
PY: Potential yield = S1 + S2 mg HC/g rock.
PI: Production Index = S1/(S1 + S2).TS: Sulfur content (wt.%).

the long-chain *n*-alkanes > C_{27} with odd over-even carbon numbers predominance indicates a land plant-derived OM [54, 55]. The chromatograms suggest that the analyzed extracts contain a diverse array of alkane compounds ranging from C_6 to C_{36} *n*-alkanes (Figure 6). The unimodal distribution and widespread dominance of short-chain/low to medium molecular weight (n-C_{13}–n-C_{20}) and (n-C_{21}–n-C_{27}) n-alkanes contrasted significantly with the long-chain *n*-alkanes (n-C_{27}–n-C_{36}) in the majority of the analyzed samples. The well extracts (A01-17-080-18W6) demonstrate a predominance of short-chain *n*-alkanes with a low molecular weight n-C_{20} (Figure 6). The most index acyclic isoprenoid hydrocarbons through concentration are Pristane (Pr) and phytane (Ph) in which they used to reflect the depositional conditions of source rocks [56]. All the studied samples show a significant amount of acyclic isoprenoids (Table 2), as demonstrated by Pr/n-C_{17} versus Ph/n-C_{18} ratios, where it is generally <1 except for a few samples from well (11-25-77-20W6) >1. The ratio of Pr/Ph has been used as an indicator of the redox conditions during deposition and diagenesis [57,

58]. The formation of Ph (C_{20}) happens when the phytol of the chlorophyll loses a hydroxyl group, which was interpreted as a reducing type environment indicator, and when the phytol loses one carbon atom, it yields Pr (C_{19}), which was interpreted to be in oxidizing environments [3, 56, 59, 60]. Within the oil window, the Pr/Ph ratios of crude oils and source rocks have a weak correlation with the depositional redox conditions [56, 58, 61].

An OM derived mainly from land plants preserved under oxidizing conditions will give high Pr/Ph > 3 ratios, while an OM of marine origin preserved under reducing conditions will provide ratios of Pr/Ph < 1, and values between 1 and 3 suggest suboxic conditions [4].

The studied extracts show high relative concentrations of pristane mostly, with ratios of Pr/Ph lies mostly between 1 and 3, suggesting a mixed marine-terrestrial input OM that was preserved under anoxic to suboxic conditions. Except for the samples from well (15-34-080-18W6) that show Pr/Ph ratio less than 1 (Table 2), However, other source
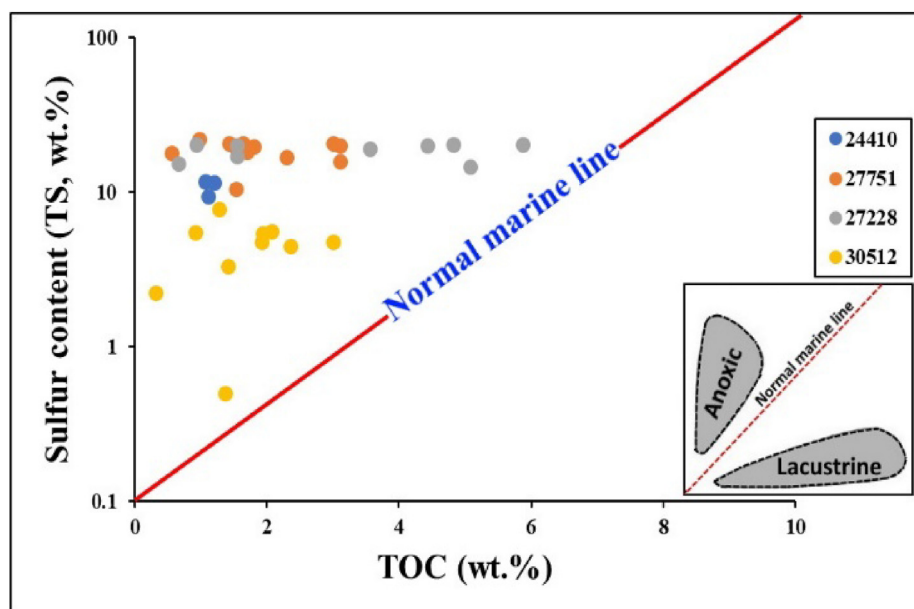
Figure 3. The cross plot of TS (wt.%) versus TOC (wt.%), showing an anoxic marine depositional environment for MF samples from all the wells (After Berner and Raiswell [43]).
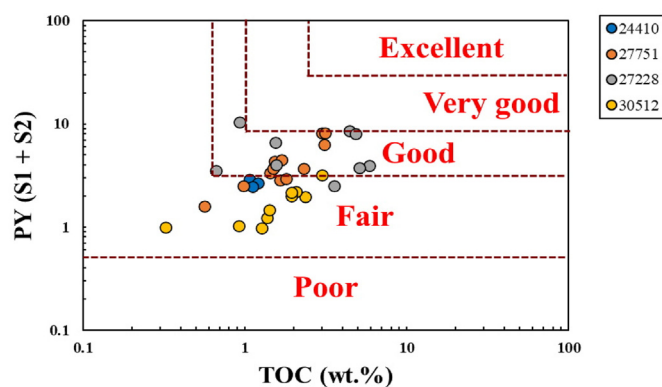

Figure 4. The relation between TOC and PY shows the generating potential of the MF source rock (After Berner and Raiswell [43]).

materials than phytol from chlorophylls [62] and thermal maturity [63] may influence the Pr/Ph ratio.

The cross-plot of Pr/n-C$_{17}$ versus Ph/n-C$_{18}$ (Figure 7) is commonly used to interpret source rock depositional environment conditions and OM type [4, 64]. Accordingly, the mixed marine and terrestrial sources of OM that was the dominant source that was deposited under anoxic to suboxic conditions, except for the samples from well (15-34-080-18W6) which is derived from marine source, deposited in an anoxic environment, and that all the samples were in the mature stage. which is also consistent with the results obtained from the cross plot of TS and TOC illustrated in (Figure 3).

The carbon preference index (CPI) of *n*-alkanes was calculated according to the formula proposed by [3], which is 2(C$_{23}$ + C$_{25}$ + C$_{27}$ + C$_{29}$)/[C$_{22}$ + 2(C$_{24}$ + C$_{26}$ + C$_{28}$)+C$_{30}$] to provide some deep understanding of the OM source and conditions during deposition. CPI value is greatly influenced by OM input. CPI <1.0 indicate reducing depositional conditions [65]. The CPI values for all the analyzed samples were around the unity (Table 2) and were plotted against the Pr/Ph ratios (Figure 8), which indicates that the OM deposited under

relatively reducing (dysoxic) conditions and is in the matured and beyond level [65].

This study calculated the waxiness index using the $\sum$(n-C$_{21}$–n-C$_{31}$)/$\sum$(n-C$_{15}$–n-C$_{20}$) ratio. This index is an indicator used to determine the terrigenous sources input in the sediments relying on the presumption that terrigenous sources contribute with high molecular weight n-alkane components [4]. Samples from MF source rock generally show medium to high waxiness index (Table 2), indicating relatively a mixed source of OM of land plant biomarkers, mainly except for the samples from well (15-34-080-18W6), which shows relatively low waxiness index suggesting a marine source. This interpretation was corroborated by the cross-plot of waxiness and Pr/Ph ratio (Figure 9).

Hopane distributions of the analyzed samples were determined based on the SIM mode m/z 191 traces (Figure 10). Peak identifications of the m/z 191 chromatographs were made based on retention times and published literature [10, 52, 60, 67, 68]. The Peak assignments are shown in Appendix A, and the calculated ratios are listed in (Table 3). For all analyzed samples, the saturated hydrocarbon m/z 191 mass chromatograms reveal that pentacyclic and tricycle terpanes are more abundant, while tetracycle terpanes are less abundant.

Hopanoids are important biomarkers indicators for bacterial-derived OM [69]. Their composition and distribution mainly consist of (H)-norhopane C$_{29}$ to C$_{35}$ 17α (H) 21β with hopanes C$_{29}\alpha\beta$ and C30$\alpha\beta$ as major compounds and are similar in most of the samples (Figure 9). However, the C$_{29}$ hopane relative abundance is generally less than that of C$_{30}$ hopane in most of the analyzed samples, with C$_{29}$/C$_{30}$17α (H)-hopane ratios average of 0.65 (Table 3). The dominance of C$_{30}$ hopane is an indicator of clay-rich source rocks [70]. The (H)-moretane 17β,21α was also detected in low concentrations in many analyzed samples.

Gammacerane is frequently used to determine the salinity-stratified water column and may indicate photic zone anoxia. It is believed to have evolved from tetrahymanol in bacterivorous ciliates that live at the interface between a high-salinity water layer and a lower-salinity upper layer [62, 71]. Gammacerane is present in low concentrations in all the

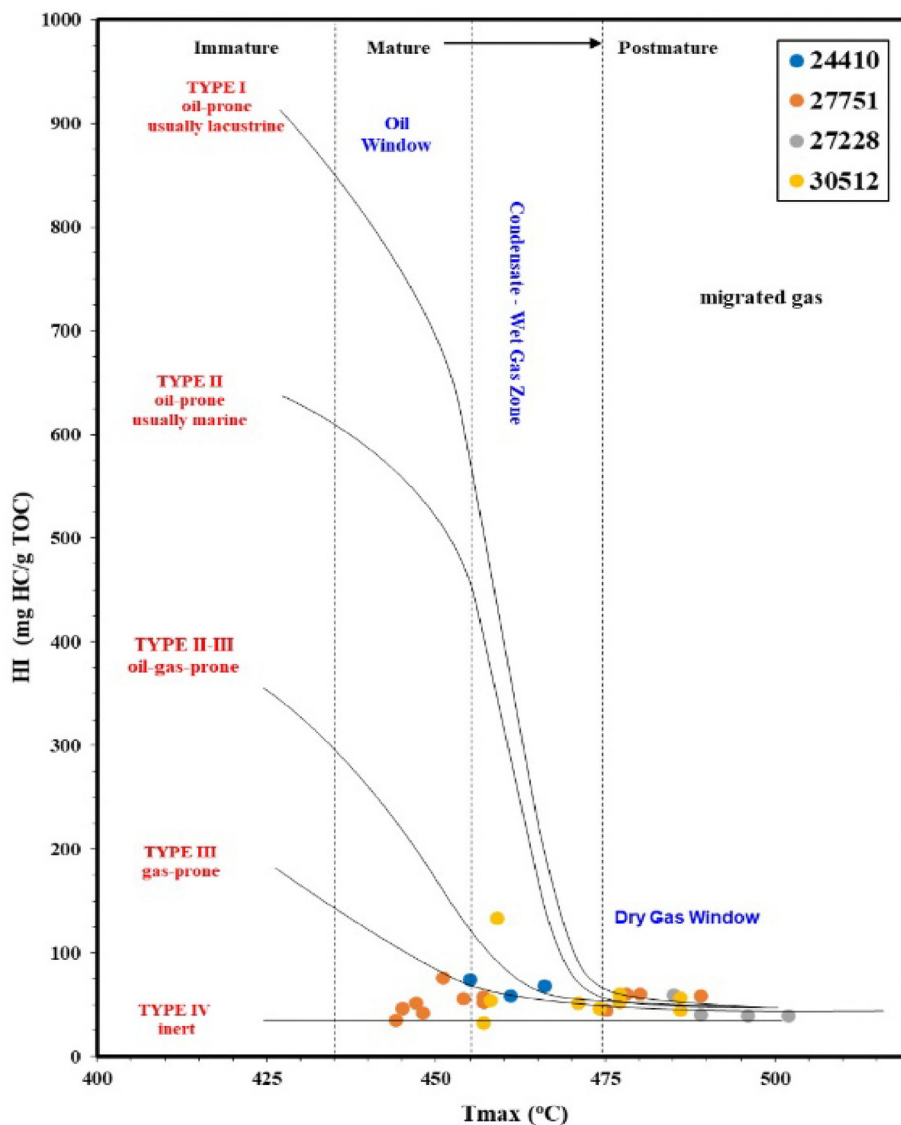**Figure 5.** HI vs Tmax on s pseudo van Krevelen graph, showing quality and maturity of the kerogen in the analyzed MF samples [49].
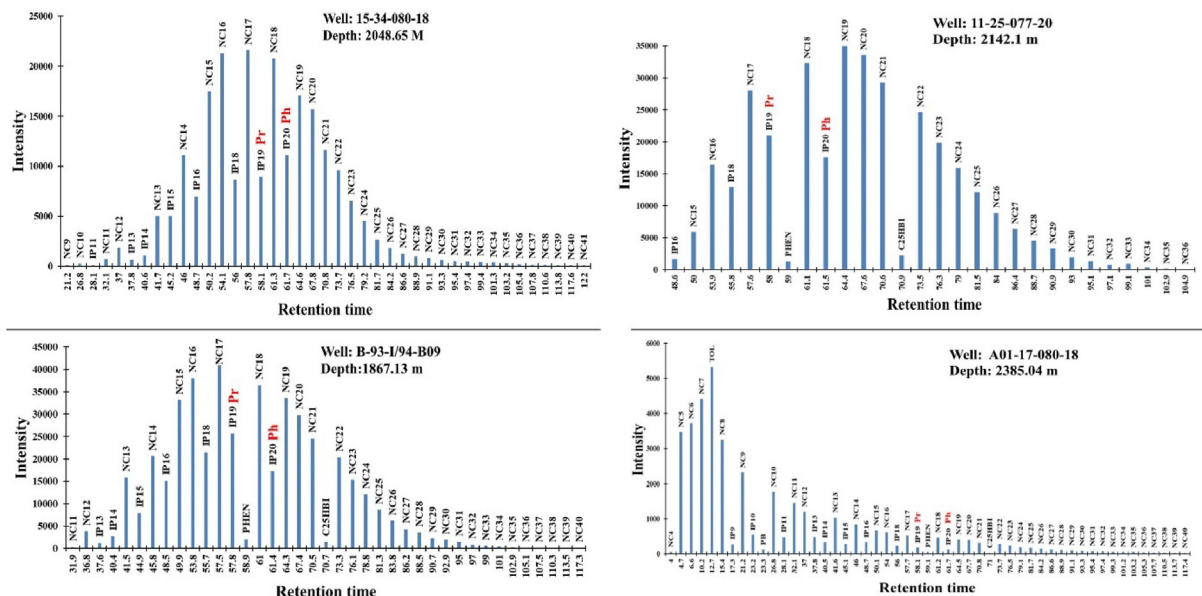

Figure 6. Mass fragmentograms of saturated hydrocarbon fractions of four representatives MF shale samples.

Table 2. Biomarker parameters of the selected MF source rock samples.

Well name	Sample Depth (m)	Pr/n-C$_{17}$	Ph/n-C$_{18}$	Pr/Ph	CPI	Waxiness
15-34-080-18W6	2048.65	0.41	0.53	0.80	1.05	0.36
	2054.93	0.44	0.54	0.81	1.04	0.35
	2060.02	0.46	0.59	0.80	1.09	0.33
b-093-I/094-B-09	1852.80	0.83	0.66	1.52	1.00	0.37
	1859.14	0.83	0.68	1.49	1.01	0.40
	1866.76	0.87	0.71	1.51	1.01	0.39
	1867.13	0.92	0.74	1.43	1.05	0.47
	1871.10	0.85	0.71	1.38	1.03	0.45
	1883.01	0.91	0.74	1.33	1.01	0.60
	1898.61	0.78	0.63	1.50	0.99	0.42
	1933.04	0.70	0.52	1.63	0.94	0.44
	1948.10	0.82	0.66	1.37	0.98	0.52
	1973.10	0.83	0.66	1.38	0.93	0.51
	1983.10	0.80	0.65	1.42	0.94	0.60
	1999.50	0.72	0.56	1.51	0.96	0.42
11-25-77-20W6	2142.10	1.11	0.83	1.16	1.05	0.85
	2148.60	0.91	1.09	0.88	1.08	0.90
	2152.00	0.57	0.55	1.76	1.02	0.54
	2159.80	0.80	0.80	1.19	1.08	1.42
	2161.80	0.42	0.29	2.25	1.09	0.39
	2163.80	1.61	1.29	0.88	1.06	1.63
	2166.60	0.56	0.47	1.89	1.06	0.66
	2168.80	1.31	1.07	1.13	1.09	0.98
	2186.60	1.13	0.98	1.21	1.09	0.90
A01-17-80-18W6	2385.04	0.48	0.41	1.36	0.99	0.60
	2392.87	0.68	0.53	1.48	0.99	0.56
	2402.17	0.66	0.52	1.49	0.95	0.59
	2411.48	0.79	0.62	1.55	0.99	0.48
	2420.67	0.73	0.57	1.54	1.01	0.47
	2429.81	0.71	0.56	1.53	1.00	0.46
	2438.76	0.69	0.53	1.60	1.00	0.43
	2447.88	0.83	0.63	1.53	1.02	0.51
	2457.33	0.53	0.40	1.60	1.00	0.43
	2465.14	0.58	0.42	1.69	1.00	0.37

Pr:pristane, Ph:phytane, Pr/Ph pristane/phytane, Pr/n-C17 pristane/n-C17, Pr/n-C18 pristane/n-C18, CPI carbon preference index [2(C23 + C25 + C27 + C29)/(C22 + 2[C24 + C26 + C28]+C30)], waxiness index $\sum$ (n-C21-n-C31)/$\sum$ (n-C15-n-C20).
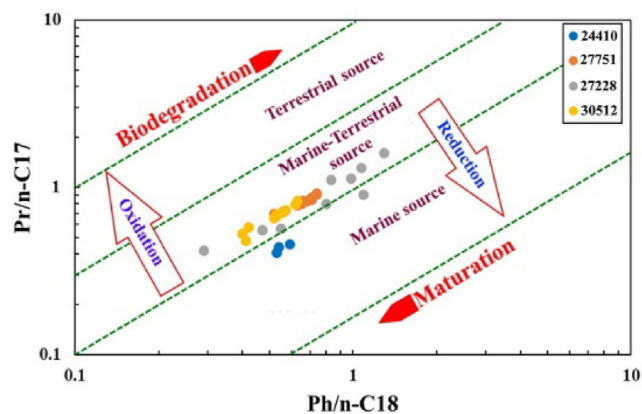

Figure 7. Plot of Pr/n-C17 vs Ph/n-C18 demonstrating the OM source, preservation conditions, and the maturity of the MF source rock [4, 64].

analyzed samples with an average index of 0.055, and this indicates a salinity water column stratification during the deposition of the MF source rock; this shows the prevailing depositional conditions of the sediments were anoxic to suboxic, reducing (dysoxic), which is supported by the interpretation from Pr/Ph ratios and the consistency of the interpretation of the high TS (Table 1).

Terpanes (tetracyclic and tricyclic) are marine environment common biomarkers and are thought to be originated from algae, especially *Tasmanites* and bacteria [72, 73, 74]. However, Abdullah [68] and Philp [10] have suggested that partial aerobic oxidation may be the source for the formation of tricyclics not in necessary *Tasmanites*. Accordingly, the diagenetic factors are considered a probable cause of their abundance in source rocks and oils than direct biosynthetic production by specific organisms [75].

According to the findings in (Table 3), tricyclic terpane concentrations are significantly higher than tetracyclic concentrations in the vast majority of the samples examined (indicated by C$_{24}$ tricyclic/C$_{24}$ tetracyclic). The relatively high C$_{23}$ tricyclic terpane concentrations in comparison with that of the C$_{24}$ tetracyclic in the analyzed MF source

rock samples may be a clue of high bacterial activities and an environmental condition that is marine (dysoxic), and also supports the assumption that the OM has been originated from algal origin under diagenetic factors [9]. The C$_{24}$/C$_{23}$ tricyclic terpanes ratio show low to medium values (Table 3) in the analyzed MF source rock samples; this is interpreted to mean that the OM is a mix of marine and terrestrial. The tricyclic terpane ratio of C$_{26}$/C$_{25}$ can be used to differentiate marine from lacustrine source rocks [9, 76]. The OM in the source rock of the MF was interpreted as mixed marine and terrigenous organic materials because of the low abundance of the C$_{26}$ tricyclic terpane in comparison with the C$_{25}$ tricyclic terpane in most of the analyzed samples (Table 3) [9, 77].

Another important biomarker group is the steranes (Table 4), which were determined based on m/z 217 traces. Appendix A contains a list of the Peak assignments. Fragmentograms for peak identification were generated using retention times and previously published literature (Figure 11) [10, 52, 60, 67, 68].

Higher plants and algae are the source of sterols which are believed to be the origin of steranes [78]. The regular steranes (C$_{27}$, C$_{28,}$ and C$_{29}$) relative proportions can vary very much from sample to sample and are influenced by the type of OM source [78], although it can be used as a paleoenvironmental condition indicator [79]. Where they suggested that the presence of C$_{27}$ steranes in predominant quantities indicates a marine phytoplankton environment mostly, while the preponderance of the amount of C$_{29}$ steranes may indicate a terrestrial environment mostly, and C$_{28}$ abundancy might indicate an intense contribution by lacustrine algae. However, Volkman, et al. [74] later noted that some marine organisms participate in C$_{29}$ steranes. Nichols, et al. [80] also noticed that marine diatoms contribute to significant amounts of C$_{29}$ sterols during the spring bloom in freezing Antarctic waters.

The analyzed samples, however, show a higher proportion of C$_{27}$ (30.3–55.9 %) and C$_{29}$ (27.7–51.1 %) steranes compared to C$_{28}$ (13.5–25 %) (Table 4), reflecting mixed aquatic and terrestrial OM [3] as illustrated by the ternary diagram of the regular sterane ratio (Figure 12A) and the cross plot of C$_{27}$/C29ααα20R sterane versus the Pr/Ph ratio (Figure 12B).

These results were consistent with the medium hopane/sterane ratios and the low to medium C$_{29}$/C$_{27}$ sterane ratios (Table 4). The Pr/Ph ratio cross-plots with both hopane/sterane and sterane C$_{27}$/(C$_{27}$ + C$_{29}$) ratios (Figure 13A, B) further support this interpretation.

The interpreted marine depositional environment and dysoxic conditions were also supported by the hopane/sterane ratios, which range from 0.52 to 1.79, and moderate diasterane/sterane ratio 1.42–3.4 in the analyzed samples. The parameters of n-alkane and biomarker maturity
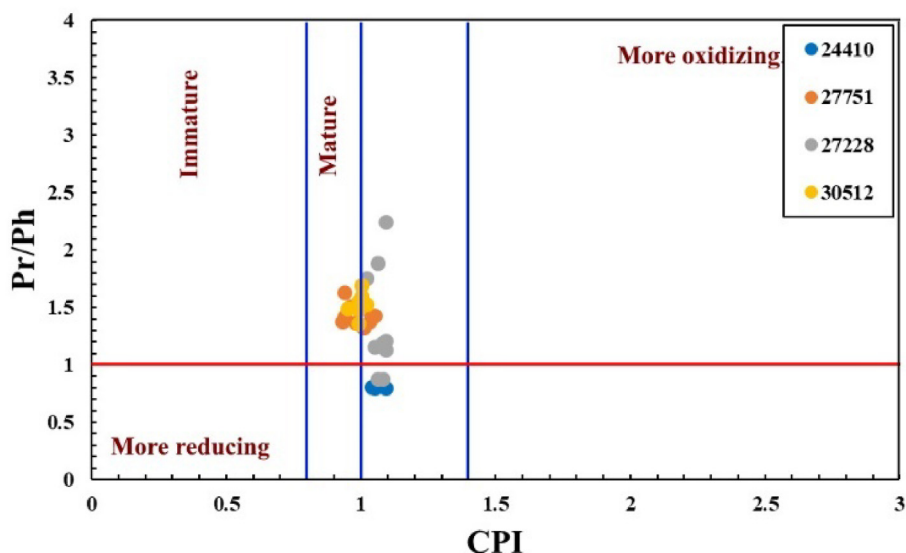
Figure 8. A cross plot of CPI versus Pr/Ph indicates the OM's preservation conditions and maturity for the studied MF samples (modified after Meyers and Snowdon [65]).

data were used in this study to assess the level of maturity of the MF source rock. The ratio of odd to even carbon numbered n-alkanes can be used to estimate the sediments' organic maturation level [3, 4, 82]. These measurements include the CPI; using the formula proposed by Peters and Moldowan [3], CPI values >1 or <1 indicate thermal immaturity, while the OM that is thermally matured has values of CPI = 1. As a result, the CPI for the analyzed samples was around unity (Table 1); this provides compelling evidence that the vast majority of the samples under investigation are thermally mature (Figure 7) [82]. All of the samples have reached a stage of maturity that is conducive to hydrocarbon production, as determined by the relationship between $Pr/n\text{-}C_{17}$ and $Ph/n\text{-}C_{18}$ (Figure 6).

The biomarker maturation parameters obtained from the m/z 191 and m/z 217 SIM mode, such as Ts/(Ts + Tm), C_{32} [22S/(22S + 22R)] homohopane, moretane/hopane and [20S/(20S + 20R)] and [ββ/(ββ+αα)] C_{29} sterane ratios, were generally used as maturity markers [67, 83]. However, the source input and thermal maturation factors and other ratios may influence the Ts/(Ts + Tm) ratio [3]. Seifert and

Moldowan [84] have related the increase in Ts to Tm ratio to the maturity increasing as the Tm is unstable compared to Ts during the catagenesis stage.

The Ts/(Ts + Tm) ratio for all the studied samples shows a range of 0.58–0.68 (Table 2); this signifies mature to postmature for all the analyzed samples. C_{31}-hopane is the most common homohopanes in all the analyzed samples. In most of the samples, S-isomers predominate over R-isomers among the homohopanes (C_{31}–C_{34}), indicating that the sample has reached its mature state. Furthermore, Seifert and Moldowan [85] discovered that the [22S/(22S + 22R)] homohopane ratio increases from 0 to 0.6 during the process of thermal maturity. But during the postmature stages, the ratio ranges from 0.57 to 0.62; these findings support the notion that the samples have progressed beyond the mature stage and have reached the postmature stage.

The [22S/(22S + 22R)] isomerization values are calculated using the C_{31} or C_{32}-homohopane results. The C_{32} [22S/(22S + 22R)] ratios for the analyzed samples range from 0.56 to 0.63, indicating thermally mature for hydrocarbon generation.
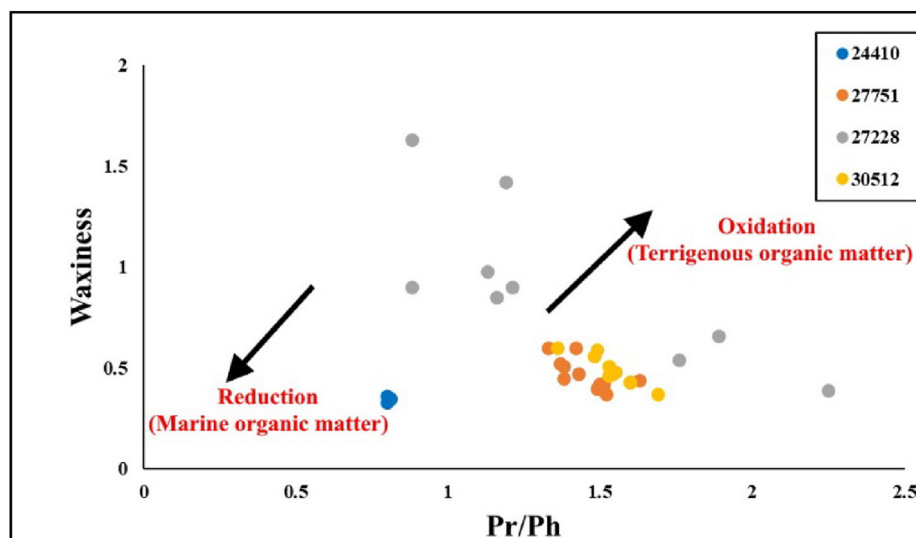

Figure 9. Waxiness index vs Pr/Ph ratio cross-plot showing the source input of the OM and depositional conditions ([66]).
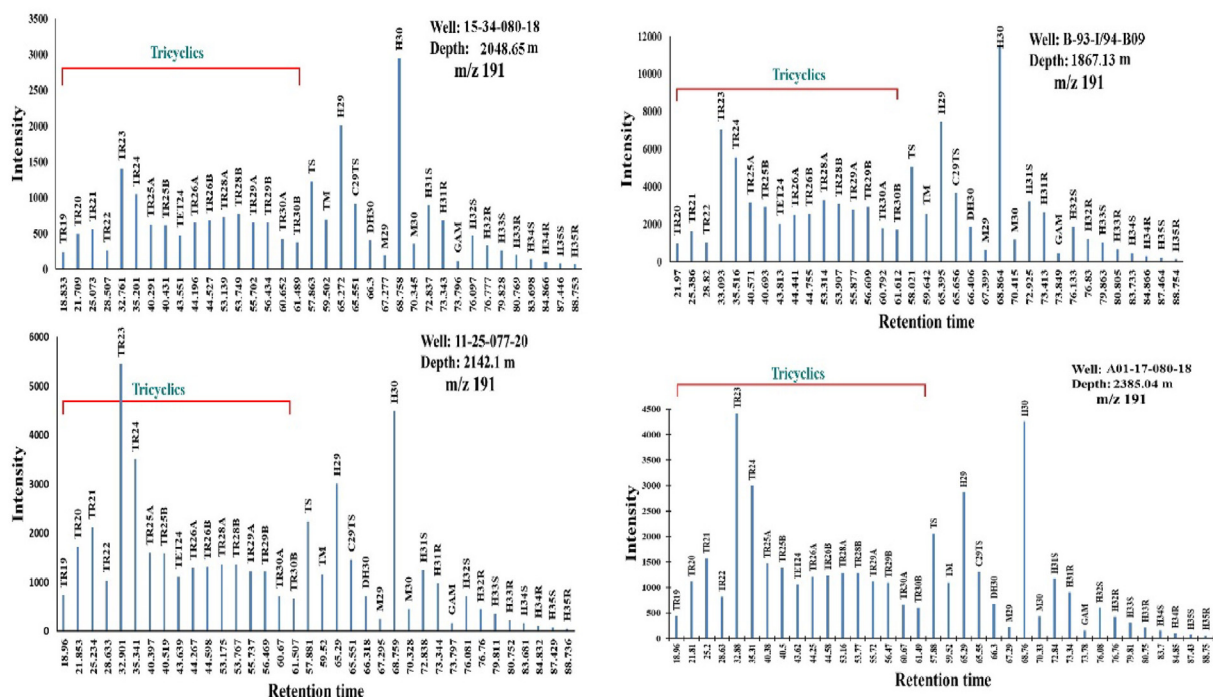
Figure 10. Mass fragmentograms measured in the SIM mode (m/z 191) of terpenoids for four samples representing the four wells from the study area.

Thermal maturity reduces the concentrations of C_{29}-hopanes and C_{30}-moretanes in comparison to the corresponding hopanes [4] because of the lower thermal stability of the C_{30}-(H) moretanes compared to the C_{29}-(H) hopanes. With increasing OM maturity, the C_{30}-M/C_{30}–H ratio decreases from about 0.8 in immature bitumen to less than 0.15 in mature source rocks and 0.05 in oils [4, 83, 85]. The

Table 3. Calculated parameters of hopanes biomarker from the SIM mode (m/z191) of the analyzed samples.

Well name	Sample depth	Hopanes (Thermal maturity)									Tricyclic (TT) and tetracyclic (TeT) terpanes (OM input & preservation conditions)			
		Tm/Ts	Ts/ (Ts + Tm)	C29H/ C30H	C30M/ C30H	C31 22S/ (22S + 22R)	C32 22S/ (22S + 22R)	C29N/ C30H	C31R/ C30H	G/ C30H	C25TT/ C26TT	C24TT/ C24TET	C24TT/ C23TT	C24TET/ C30H
15-34-080-18W6	2048.65	0.52	0.58	0.62	0.14	0.49	0.56	0.58	0.27	0.07	1.27	3.86	0.63	0.28
	2054.93	0.51	0.59	0.65	0.12	0.52	0.57	0.55	0.25	0.05	1.23	1.74	0.45	0.24
	2060.02	0.49	0.58	0.69	0.13	0.55	0.62	0.60	0.27	0.06	1.28	3.56	44.0	0.24
B-93-I/94-B09	1852.80	0.52	0.58	0.62	0.14	0.49	0.56	0.62	0.25	0.07	1.49	3.21	0.55	0.22
	1859.14	0.51	0.59	0.65	0.12	0.52	0.57	0.55	0.27	0.05	1.37	3.19	0.54	0.18
	1866.76	0.49	0.58	0.69	0.13	0.55	0.62	0.52	0.26	0.07	2.86	4.72	0.61	0.26
	1867.13	0.50	0.63	0.67	0.12	0.53	0.60	0.64	0.28	0.06	1.06	3.21	0.63	0.18
	1871.10	0.51	0.62	0.64	0.11	0.55	0.63	0.68	0.27	0.04	1.18	3.51	0.58	0.18
	1883.01	0.51	0.61	0.65	0.11	0.54	0.61	0.61	0.27	0.04	1.25	4.93	0.60	0.22
	1898.61	0.50	0.64	0.60	0.12	0.54	0.61	0.57	0.26	0.04	1.56	2.06	0.38	0.21
	1933.04	0.48	0.68	0.63	0.13	0.50	0.57	0.63	0.25	0.06	1.61	3.89	0.43	0.24
	1948.10	0.50	0.67	0.64	0.14	0.51	0.58	0.60	0.26	0.07	1.67	3.38	0.49	0.24
	1973.10	0.48	0.68	0.63	0.13	0.51	0.58	0.67	0.26	0.06	1.61	3.76	0.55	0.19
	1983.10	0.50	0.66	0.64	0.13	0.50	0.56	0.62	0.25	0.06	1.68	2.49	0.62	0.18
	1999.50	0.49	0.67	0.60	0.12	0.51	0.59	0.59	0.25	0.05	1.25	3.20	0.61	0.23
11-25-077-20W6	2142.10	0.51	0.66	0.66	0.11	0.53	0.60	0.66	0.29	0.04	1.12	3.80	0.62	0.24
	2148.60	0.49	0.67	0.66	0.12	0.52	0.59	0.66	0.26	0.05	1.01	1.52	0.62	0.24
	2152.00	0.53	0.65	0.67	0.13	0.52	0.61	0.67	0.28	0.05	0.85	3.13	0.72	0.19
	2159.80	0.50	0.67	0.65	0.11	0.52	0.62	0.65	0.26	0.05	0.99	2.70	0.70	0.21
	2161.80	0.52	0.66	0.67	0.12	0.54	0.58	0.67	0.26	0.05	0.98	2.79	0.67	0.19
	2163.80	0.50	0.67	0.65	0.11	0.51	0.61	0.65	0.27	0.05	1.06	3.34	0.66	0.20
	2166.60	0.51	0.66	0.65	0.11	0.53	0.61	0.65	0.25	0.04	0.95	3.10	0.75	0.18
	2168.80	0.55	0.65	0.66	0.12	0.53	0.58	0.66	0.25	0.04	1.16	3.20	0.61	0.25
	2186.60	0.49	0.67	0.67	0.11	0.52	0.59	0.67	0.25	0.04	1.07	3.40	0.63	0.27

Table 3 (*continued*)

Well name	Sample depth	Hopanes (Thermal maturity)									Tricyclic (TT) and tetracyclic (TeT) terpanes (OM input & preservation conditions)			
		Tm/Ts	Ts/ (Ts + Tm)	C29H/ C30H	C30M/ C30H	C31 22S/ (22S + 22R)	C32 22S/ (22S + 22R)	C29N/ C30H	C31R/ C30H	G/ C30H	C25TT/ C26TT	C24TT/ C24TET	C24TT/ C23TT	C24TET/ C30H
A01-17-080-18W6	2385.04	0.53	0.68	0.65	0.14	0.52	0.59	0.63	0.28	0.07	1.09	3.77	0.58	0.21
	2392.87	0.54	0.67	0.65	0.14	0.53	0.60	0.65	0.29	0.07	1.12	1.63	0.60	0.19
	2402.17	0.52	0.68	0.66	0.13	0.53	0.60	0.63	0.27	0.06	1.13	3.41	0.61	0.21
	2411.48	0.53	0.66	0.67	0.13	0.54	0.62	0.67	0.27	0.06	1.23	3.04	0.61	0.23
	2420.67	0.53	0.67	0.65	0.14	0.53	0.59	0.64	0.28	0.04	1.09	2.90	0.63	0.22
	2429.81	0.51	0.66	0.65	0.12	0.52	0.60	0.65	0.29	0.05	1.10	2.91	0.62	0.22
	2438.76	0.51	0.67	0.66	0.12	0.54	0.61	0.66	0.28	0.04	1.06	3.87	0.61	0.20
	2447.88	0.52	0.65	0.67	0.11	0.55	0.62	0.63	0.28	0.05	1.05	2.85	0.59	0.20
	2457.33	0.53	0.64	0.66	0.11	0.54	0.60	0.67	0.27	0.05	1.05	3.33	0.60	0.21
	2465.14	0.52	0.63	0.65	0.12	0.53	0.60	0.64	0.26	0.07	1.07	3.56	0.62	0.19

C29/C30: C29 norhopane/C30hopane. C31R/C30 = C31 regular homohopane/C30 hopane. G/C30: Gammacerane/C30 hopane. C30M/C30H = C30 moretane/C30 hopane. Ts: (C27 18α(H)-22,29,30-trisnorneohopane). Tm: (C27 17α(H)-22,29,30-trisnorhopane).

values obtained for the analyzed MF source rock samples lie in the range of 0.11–0.14 and suggest that they are postmature between the oil to the dry gas windows; this corresponds to the previous maturity results above.

Diasteranes are present in considerable amounts in most of the analyzed samples (Figure 10). Diasteranes are believed to be more stable than steranes at high thermal maturity, and they are believed to be produced during diagenesis and early catagenesis by the transformation of sterols [3, 9]. These maturation interpretations were supported by the diasterane/regular sterane ratios calculated from the mass fragmentograms of the 217 ion m/z. The ratio of diasterane to sterane in the analyzed samples ranges from 1.42 to 3.4, indicating that the majority of the samples are mature in terms of hydrocarbon generation. The C_{29}-5α, 14α,17α(H)-[20S/(20S + 20R)] and the [ββ/(ββ+αα)] for C_{29} steranes are other parameters calculated from the same ion mass fragmentograms

for evaluating the maturity level these ratios are believed to increase with increasing thermal maturity [9]. Gallegos and Moldowan [86] proposed that the steranes C_{29} [20S/(20S + 20R)] ratio equilibrates at 0.52 to 0.55; These numbers, however, are likely exaggerated, with the actual value being closer to 0.5 in oils and source rocks. They reported that other C_{29} sterane isomers usually contaminate the peak corresponding to the C_{29}ααα20S isomer. On the other hand, the lithofacies types may affect the ββ/(ββ+αα) [3, 87]. According to Korkmaz and Gülbay [88], some of the inconsistencies in the extent of sterane isomerization can be attributed to other factors such as organic facies, environment, and lithology, so the values may not be wholly equilibrated. The ranges of the 20S/(20S + 20R) and ββ/(ββ+αα) values for the MF source rock samples are 0.4–0.65 and 0.44 to 0.64, respectively; these values indicate that the analyzed samples are thermally mature enough to generate hydrocarbons (Table 4).
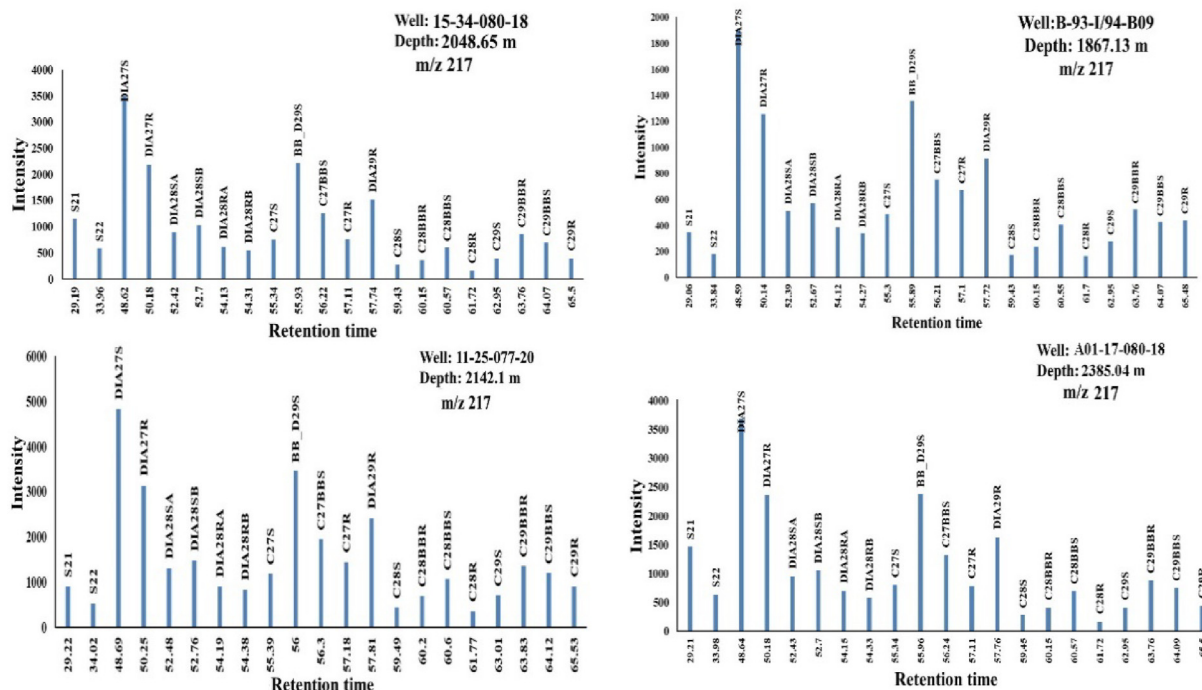

Figure 11. M/z 217 mass fragmentogram measured in SIM mode of sterane hydrocarbon fractions of the four MF source rock samples.

Table 4. Parameters for the sterane biomarker derived from the m/z 217 fragmentograms of the analyzed samples.

Sample ID	Depth (m)	Thermal maturity		Source input and depositional conditions						
		Ster-C_{29} 20S/(20S + 20R)	Ster-C_{29} $\beta\beta/(\beta\beta+ \alpha\alpha)$	Regular steranes (%)			$C_{27}/(C_{27} + C_{29})$	Ster-C_{27}/Ster-C_{29}	Hop/Ster	Diaste/Ster
				%C_{27}	%C_{28}	%C_{29}				
15-34-080-18W6	2048.65	0.46	0.51	50.6	21.1	28.3	0.64	1.79	1.79	1.42
	2054.93	0.49	0.52	53.4	18.9	27.7	0.66	1.93	1.75	1.9
	2060.02	0.44	0.53	51.6	20.3	28.1	0.65	1.84	1.56	1.6
B-93-I/94-B09	1852.8	0.48	0.56	31.0	19.0	50.0	0.38	0.62	0.67	2.34
	1859.14	0.45	0.53	40.8	18.2	41.0	0.5	1	0.65	3.01
	1866.76	0.40	0.44	30.3	20.7	49.0	0.38	0.62	0.63	2.21
	1867.13	0.45	0.51	30.7	24.0	45.3	0.4	0.68	0.66	2.36
	1871.1	0.43	0.48	31.4	25.0	43.6	0.42	0.72	0.66	2.46
	1883.01	0.51	0.57	30.9	22.9	46.2	0.4	0.67	0.68	3.11
	1898.61	0.46	0.54	31.4	18.5	50.1	0.39	0.63	0.65	2.29
	1933.04	0.45	0.52	34.4	17.3	48.3	0.42	0.71	0.65	3
	1948.1	0.48	0.57	34.6	17.8	47.6	0.42	0.73	0.65	2.89
	1973.1	0.45	0.51	32.0	16.9	51.1	0.39	0.63	0.69	2.46
	1983.1	0.43	0.48	34.4	16.4	49.2	0.41	0.7	0.69	2.56
	1999.5	0.51	0.57	38.0	15.1	46.9	0.45	0.81	0.67	3.4
11-25-077-20W6	2142.1	0.55	0.61	40.0	15.3	44.7	0.47	0.89	0.67	3.34
	2148.6	0.50	0.58	41.1	15.4	43.5	0.49	0.94	0.67	2.82
	2152	0.45	0.49	41.8	16.1	42.1	0.5	0.99	0.71	2.05
	2159.8	0.50	0.56	43.1	16.9	40.0	0.52	1.08	0.69	2.46
	2161.8	0.48	0.53	44.0	16.4	39.6	0.53	1.11	0.69	2.56
	2163.8	0.56	0.62	46.7	15.1	38.2	0.55	1.22	0.67	3.4
	2166.6	0.51	0.59	55.9	13.5	30.6	0.65	1.83	0.65	2.18
	2168.8	0.50	0.57	43.6	17.3	39.1	0.53	1.12	0.66	2.8
	2186.6	0.53	0.62	47.8	16.6	35.6	0.57	1.34	0.65	3.09
A01-17-080-18W6	2385.04	0.63	0.62	33.8	17.9	48.3	0.41	0.7	0.66	2.25
	2392.87	0.65	0.64	33.8	17.0	49.2	0.41	0.69	0.67	3.18
	2402.17	0.62	0.61	31.6	21.1	47.3	0.4	0.67	0.66	2.05
	2411.48	0.60	0.59	37.9	19.6	42.5	0.47	0.89	0.68	2.31
	2420.67	0.59	0.58	31.1	19.8	49.1	0.39	0.63	0.66	2.38
	2429.81	0.60	0.59	32.9	20.0	47.1	0.41	0.7	0.68	2.15
	2438.76	0.65	0.64	33.7	21.3	45.0	0.43	0.75	0.69	3.05
	2447.88	0.62	0.61	35.2	22.2	42.6	0.45	0.83	0.52	2.86
	2457.33	0.62	0.61	39.8	20.3	39.9	0.5	1	0.53	2.65
	2465.14	0.63	0.62	39.6	19.4	41.0	0.49	0.97	0.56	2.48
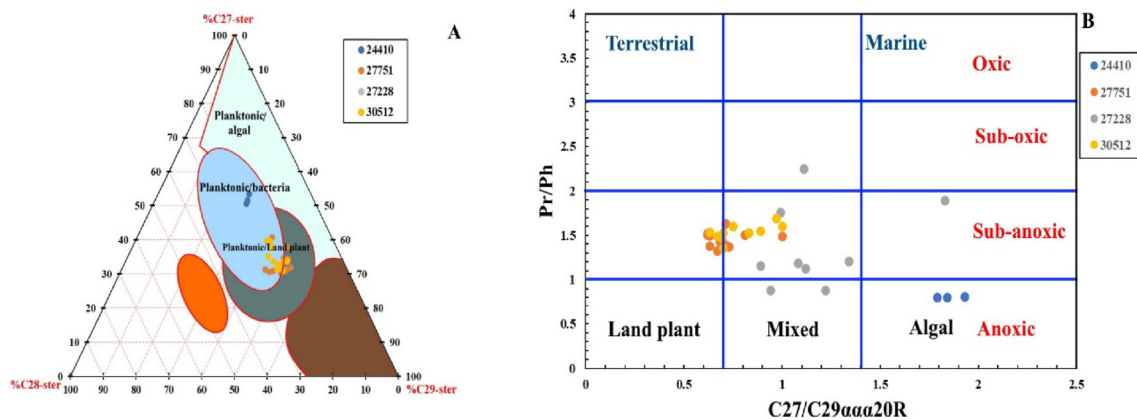
Figure 12. A: a ternary diagram of C_{27}, C_{28}, and C_{29} $\alpha\alpha\alpha$ 20R steranes; B: Cross plot of C_{27}/C_{29} $\alpha\alpha\alpha$ 20R sterane ratio versus Pr/Ph ratio, showing the depositional environment and OM type of MF source rock (modified after Huang and Meinschein [79]).
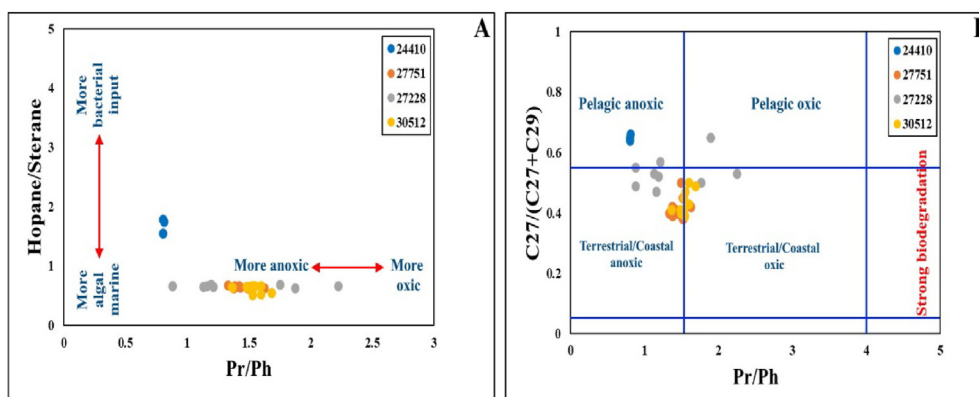
Figure 13. A: Cross-plot of Hopanes/Steranes vs Pr/Ph ratios; B: Cross-plot of $C_{27}/(C_{27} + C_{29})$ regular steranes vs Pr/Ph ratios showing depositional environment conditions and source input [81].

5. Conclusions

The source rock of the MF in the northeastern part of the BC area, Canada, was analyzed using bulk organic geochemical methods. The results achieved in this study give strong indications as follows:

1. The MF is organically good to very good source rock with an average TOC of 2.1 wt.%. Moreover, the high TS > 2 wt.% in the MF source rock indicates low oxygen deposition in a marine environment.
2. A mixed marine and terrestrial OM source input for MF source rock was deduced by the prevalence of the short-chain *n*-alkanes, CPI around unity, and high concentration of tricyclic terpanes and C_{24} tri/ C_{24} tetra and low hopane/sterane ratios. In addition, the cross-plots of Pr/n-C_{17} versus Ph/n-C_{18}, as well as the ternary diagram showing the relationship between regular sterane compositions, both found similar results, suggesting that the sediments studied had a mix of marine and terrigenous OM input.
3. The OM influx indicates that more marine input was toward the northeastern part, while mixed input was toward the southwestern region.
4. Dysoxic conditions were the dominant conditions during the OM deposition.
5. The waxiness index gives evidence of the terrigenous organic materials influx during the deposition of the MF source rock.
6. Different biomarker maturity data indicated that the source rock of the MF had reached the maturity stages of hydrocarbon generation.

Declarations

Author contribution statement

Azzam Barham: Conceived and designed the experiments; Performed the experiments; Analyzed and interpreted the data;

Contributed reagents, materials, analysis tools or data; Wrote the paper.

Mohd Ismail: Conceived and designed the experiments; Analyzed and interpreted the data; Wrote the paper.

Maman Hermana: Conceived and designed the experiments; Analyzed and interpreted the data; Contributed reagents, materials, analysis tools or data.

N.S. Zainal Abidi: Conceived and designed the experiments; Performed the experiments; Analyzed and interpreted the data; Contributed reagents, materials, analysis tools or data.

Data availability statement

Data will be made available on request.

Declaration of interests statement

The authors declare no conflict of interest.

Additional information

No additional information is available for this paper.

Appendix A. Peak designations for alkane hydrocarbons in saturated fraction gas chromatograms in the m/z 191 and 217 mass fragmentograms.

m/z 191			m/z 217		
Abbreviation	Compound	Peak no.	Abbreviation	Compound	Peak no.
TR C21	C21 Tricyclic (Cheilanthane)	C21	S21	C21 sterane	C21
Tri C22	C22 Tricyclic (Cheilanthane)	C22	S22	C22 sterane	C22
Tri C23	C23 Tricyclic (Cheilanthane)	C23	DIA27S	C27 βα 20S diasterane	C27
Tri C24	C24 Tricyclic (Cheilanthane)	C24	DIA27R	C27 βα 20R diasterane	C27
Tetra C24	C24 Tetracyclic	C24	DIA28SA	C28 βα 20S diasterane (a)	C28

(continued on next column)

(*continued*)

m/z 191			m/z 217		
Abbreviation	Compound	Peak no.	Abbreviation	Compound	Peak no.
Tri C25	C25 Tricyclic (Cheilanthane)	C25	DIA28SB	C28 βα 20S diasterane (b)	C28
Tri C26	C26 Tricyclic (Cheilanthane)	C26	DIA28RA	C28 βα 20R diasterane (a)	C28
Ts	18α (H),22,29,30-trisnorneohopane	Ts	DIA28RB	C28 βα 20R diasterane (b)	C28
Tm	17 α (H),22,29,30-trisnorhopane	Tm	C27S	C27 αα 20S sterane (+5 βαα)	C27
C29 hop	17 α,21 β (H)-nor-hopane	C29	BB_D29S	C27 ββ 20R + C29 dia20S	C27
C29Mor	17β(H),21α(H)-hopane (moretane)	29M	C27BBS	C27 ββ 20S sterane	C27
Hopane	17α,21 β (H)-hopane	C30	C27R	C27 αα 20R sterane	C27
C30Mor	17 β,21α (H)-Moretane	30M	DIA29R	C29 βα 20R diasterane	C29
C31(22S)	17α,21 β (H)-homohopane (22S)	31S	C28S	C28 αα 20S sterane	C28
C31 (22R)	17α,21 β (H)-homohopane (22R)	31R	C28BBR	C28 ββ 20R sterane (+5 βαα)	C28
C32(22S)	17α,21 β (H)-homohopane (22S)	32S	C28BBS	C28 ββ 20S sterane	C28
C32 (22R)	17α,21 β (H)-homohopane (22R)	32R	C28R	C28 αα 20R sterane	C28
C33(22S)	17α,21 β (H)-homohopane (22S)	33S	C29S	C29 αα 20S sterane	C29
C33 (22R)	17α,21 β (H)-homohopane (22R)	33R	C29BBR	C29 ββ 20R sterane (+5 βαα)	C29
C34(22S)	17α,21 β (H)-homohopane (22S)	34S	C29BBS	C29 ββ 20S sterane	C29
C34 (22R)	17α,21 β (H)-homohopane (22R)	34R	C29R	C29 αα 20R sterane	C29
C35(22S)	17α,21 β (H)-homohopane (22S)	35S			
C35 (22R)	17α,21 β (H)-homohopane (22R)	35R			

References

[1] N.E. Board, Canada's Energy Future 2013, Energy Supply and Demand Projections to 2035, National Energy Board, report, 2013, p. 87. https://www.neb-one.gc.ca/nrg/ntgrtd/ftr/2013/2013nrgftr-eng.pdf.

[2] J.P. Zonneveld, R.B. MacNaughton, J. Utting, T.W. Beatty, S.G. Pemberton, C.M. Henderson, Sedimentology and ichnology of the lower triassic Montney formation in the pedigree-ring/border-kahntah river area, northwestern alberta and northeastern British Columbia," (in English), Bull. Can. Petrol. Geol. 58 (2) (Jun 2010) 115–140.

[3] K.E. Peters, J.M. Moldowan, The Biomarker Guide: Interpreting Molecular Fossils in Petroleum and Ancient Sediments, 1993.

[4] K.E. Peters, K.E. Peters, C.C. Walters, J. Moldowan, The Biomarker Guide, Cambridge University Press, 2005.

[5] D. Karlsen, et al., Petroleum geochemistry of the Haltenbanken, Norwegian continental shelf, Geol. Soc. Lond. Spec. Publ. 86 (1) (1995) 203–256.

[6] S. Larter, A. Aplin, Reservoir geochemistry: methods, applications and opportunities, Geol. Soc. Lond. Spec. Publ. 86 (1) (1995) 5–32.

[7] A. Huc, Petroleum geochemistry at the dawn of the 21st century, Oil Gas Sci. Technol. 58 (2) (2003) 233–241.

[8] C. Yang, et al., Chemical fingerprints of crude oils and petroleum products, Oil Spill Sci. Technol. 2 (2017) 209–298.

[9] K. Peters, C. Walters, J. Moldowan, Book review:the biomarker guide, J. Paleolimnol. 34 (4) (2005 2005) 539–540.

[10] R.P. Philp, Biological markers in fossil fuel production, Mass Spectrom. Rev. 4 (1) (1985) 1–54.

[11] J.M. Hunt, Petroleum Geochemistry and Geology, 1995.

[12] B. Tissot, D. Welte, Petroleum Formation and Occurrence, second ed., Springer, Berlin, 1984, p. 699.

[13] N. Board, The Ultimate Potential for Unconventional Petroleum from the Montney Formation of British Columbia and Alberta, Technical report, 2013.

[14] S.D. Killops, V.J. Killops, Introduction to Organic Geochemistry, John Wiley & Sons, 2013.

[15] C. Riediger, P. Brooks, M. Fowler, L. Snowdon, Lower and Middle Triassic source rocks, thermal maturation, and oil-source rock correlations in the Peace River Embayment area, Alberta and British Columbia, Bull. Can. Petrol. Geol. 38 (1) (1990) 218–235.

[16] D. Gibson, J. Barclay, Middle Absaroka Sequence the Triassic Stable Craton, 1989.

[17] J. Barclay, F. Krause, R. Campbell, J. Utting, Dynamic casting and growth faulting: dawson Creek graben complex, Carboniferous-Permian Peace River embayment, western Canada, Bull. Can. Petrol. Geol. 38 (1) (1990) 115–145.

[18] G.R. Davies, The Triassic of the Western Canada Sedimentary Basin: tectonic and stratigraphic framework, paleogeography, paleoclimate and biota, Bull. Can. Petrol. Geol. 45 (4) (1997) 434–460.

[19] M. Orchard, E. Tozer, Triassic conodont biochronology, its calibration with the ammonoid standard, and a biostratigraphic summary for the Western Canada Sedimentary Basin, Bull. Can. Petrol. Geol. 45 (4) (1997) 675–692.

[20] J.-P. Zonneveld, M. Gingras, S. Pemberton, Trace fossil assemblages in a Middle Triassic mixed siliciclastic-carbonate marginal marine depositional system, British Columbia, Palaeogeogr. Palaeoclimatol. Palaeoecol. 166 (3-4) (2001) 249–276.

[21] J. Podruski, et al., Conventional Oil Resources of Western Canada: Geol, Survey Canada Paper, 1988, pp. 26–87.

[22] D. Edwards, J. Barclay, D. Gibson, G. Kvill, E. Halton, Triassic strata of the Western Canada sedimentary basin, Bull. Can. Petrol. Geol. 38 (1) (1990), 163-163.

[23] D. Gibson, D. Edwards, An overview of Triassic stratigraphy and depositional environments in the Rocky Mountain foothills and western interior plains, Peace River arch area, northeastern British Columbia, Bull. Can. Petrol. Geol. 38 (1) (1990) 146–158.

[24] T.F. Moslow, G.R. Davies, Turbidite reservoir facies in the lower triassic Montney formation, west-central alberta, Bull. Can. Petrol. Geol. 45 (4) (1997) 507–536.

[25] D.R. Kendall, Sedimentology and Stratigraphy of the Lower Triassic Montney Formation, Peace River basin, Subsurface of Northwestern Alberta, University of Calgary, 1999.

[26] G.R. Davies, The triassic of the western Canada Sedimentary Basin: tectonic and stratigraphic framework, palaeogeography, paleoclimate and biota, in: Triassic of the Western Canada Sedimentary Basin.," Bulletin of Canadian Petroleum Geology, 45, 1997, pp. 434–460.

[27] J.-P. Zonneveld, M. Golding, T.F. Moslow, M.J. Orchard, T. Playter, N. Wilson, Depositional Framework of the Lower Triassic Montney Formation, West-central Alberta and north-eastern British Columbia, CSPG CSEG CWLS Convention, 2011, pp. 1–4.

[28] J.-P. Zonneveld, T.F. Moslow, Palaeogeographic setting, lithostratigraphy, and sedimentary framework of the lower triassic Montney formation of western alberta and northeastern British Columbia, Bull. Can. Petrol. Geol. 66 (1) (2018) 93–127.

[29] D.M. Raup, Size of the Permo-Triassic bottleneck and its evolutionary implications, Science 206 (4415) (1979) 217–218.

[30] D.H. Erwin, Extinction: How Life on Earth Nearly Ended 250 Million Years Ago, Princeton University Press, 2006.

[31] A.D. Woods, D.J. Bottjer, F.A. Corsetti, Calcium carbonate seafloor precipitates from the outer shelf to slope facies of the Lower Triassic (Smithian-Spathian) Union Wash Formation, California, USA: sedimentology and palaeobiologic significance, Palaeogeogr. Palaeoclimatol. Palaeoecol. 252 (1-2) (2007) 281–290.

[32] J.-P. Zonneveld, M.K. Gingras, T.W. Beatty, Diverse ichnofossil assemblages following the PT mass extinction, Lower Triassic, Alberta and British Columbia, Canada: evidence for shallow marine refugia on the northwestern coast of Pangaea, Palaios 25 (6) (2010) 368–392.

[33] T.L. Playter, Petrographic and X-ray Microtomographic Analysis of the Upper Montney Formation, Northeastern British Columbia, Canada, University of Alberta (Canada), 2013.

[34] G.R. Davies, T.F. Moslow, M.D. Sherwin, The lower Triassic Montney formation, west-central Alberta, Bull. Can. Petrol. Geol. 45 (4) (1997) 474–505.

[35] T.F. Moslow, Reservoir architecture of a fine-grained turbidite system: lower triassic Montney formation, western Canada Sedimentary Basin, in: P. Weimer, R.M. Slatt, J. Coleman, N.C. Rosen, H. Nelson, A.H. Bouma, M.J. Styzen, D.T. Lawrence (Eds.), Deep-water Reservoirs of the World, Conference Proceedings, Gulf Coast SEPM, 2000, pp. 686–713.

[36] J. Utting, J. Zonneveld, R. MacNaughton, K. Fallas, Palynostratigraphy, lithostratigraphy and thermal maturity of the lower triassic toad and grayling, and Montney formations of western Canada, and comparisons with coeval rocks of the sverdrup basin, nunavut, Bull. Can. Petrol. Geol. 53 (1) (2005) 5–24.

[37] E. Scalan, J. Smith, An improved measure of the odd-even predominance in the normal alkanes of sediment extracts and petroleum, Geochimica et Cosmochimica Acta 34 (5) (1970) 611–620.

[38] C. Kelly, R. Law, H. Emerson, Methods for Analysis for Hydrocarbons and Polycyclic Aromatic Hydrocarbons (PAH) in marine Samples, CEFAS, 2000.

[39] A. El Nemr, A. El-Sikaily, A. Khaled, T.O. Said, A.M. Abd-Alla, Determination of hydrocarbons in mussels from the Egyptian Red Sea coast, Environ. Monit. Assess. 96 (1-3) (2004) 251–261.

[40] M. Talbot, The origins of lacustrine oil source rocks: evidence from the lakes of tropical Africa, Geol. Soc. Lond. Spec. Publ. 40 (1) (1988) 29–43.

[41] T.A. Schwarzkopf, Model for prediction of organic carbon in possible source rocks, Mar. Petrol. Geol. 10 (5) (1993) 478–492.

[42] I.M. Mohialdeen, M.H. Hakimi, Geochemical characterisation of Tithonian–Berriasian Chia Gara organic-rich rocks in northern Iraq with an emphasis on organic matter enrichment and the relationship to the bioproductivity and anoxia conditions, J. Asian Earth Sci. 116 (2016) 181–197.

[43] R.A. Berner, R. Raiswell, Burial of organic carbon and pyrite sulfur in sediments over Phanerozoic time: a new theory, Geochimica et Cosmochimica Acta 47 (5) (1983) 855–862.

[44] R.A. Berner, Sedimentary pyrite formation: an update, Geochimica et cosmochimica Acta 48 (4) (1984) 605–615.

[45] H. Huang, M.J. Pearson, Source rock palaeoenvironments and controls on the distribution of dibenzothiophenes in lacustrine crude oils, Bohai Bay Basin, eastern China, Org. Geochem. 30 (11) (1999) 1455–1470.

[46] R. Sykes, Peat biomass and early diagenetic controls on the paraffinic oil potential of humic coals, Canterbury Basin, New Zealand, Petrol. Geosci. 10 (4) (2004) 283–303.

[47] J.M. Wood, H. Sanei, M.E. Curtis, C.R. Clarkson, Solid bitumen as a determinant of reservoir quality in an unconventional tight gas siltstone play, Int. J. Coal Geol. 150 (2015) 287–295.

[48] K.E. Peters, M.R. Cassa, Applied Source Rock Geochemistry: Chapter 5: Part II, Essential elements, 1994.

[49] J. Espitalie, G. Deroo, F. Marquis, Rock-Eval pyrolysis and its applications, Revue De L Institut Francais Du Petrole 40 (5) (1985) 563–579.

[50] J.E. Zumberge, Prediction of source rock characteristics based on terpane biomarkers in crude oils: a multivariate statistical approach, Geochimica et Cosmochimica Acta 51 (6) (1987) 1625–1637.

[51] Z. Wang, S.A. Stout, M. Fingas, Forensic fingerprinting of biomarkers for oil spill characterization and source identification, Environ. Forensics 7 (2) (2006) 105–146.

[52] M.H. Hakimi, W.H. Abdullah, M.R. Shalaby, Molecular composition and organic petrographic characterization of Madbi source rocks from the Kharir Oilfield of the Masila Basin (Yemen): palaeoenvironmental and maturity interpretation, Arab. J. Geosci. 5 (4) (2012) 817–831.

[53] M.M. Walsh, Biomarkers for Identifying and Quantitating Oil Residues in the Environment, 2000.

[54] P. Cranwell, G. Eglinton, N. Robinson, Lipids of aquatic organisms as potential contributors to lacustrine sediments—II, Org. Geochem. 11 (6) (1987) 513–527.

[55] G. Eglinton, R.J. Hamilton, Leaf epicuticular waxes, Science 156 (3780) (1967) 1322–1335.

[56] T. Powell, D. McKirdy, Relationship between ratio of pristane to phytane, crude oil composition and geological environment in Australia, Nat. Phys. Sci. 243 (124) (1973) 37–39.

[57] K. Chandra, C. Mishra, U. Samanta, A. Gupta, K. Mehrotra, Correlation of different maturity parameters in the Ahmedabad-Mehsana block of the Cambay basin, Org. Geochem. 21 (3-4) (1994) 313–321.

[58] B. Didyk, B. Simoneit, S.t. Brassell, G. Eglinton, Organic geochemical indicators of palaeoenvironmental conditions of sedimentation, Nature 272 (5650) (1978) 216–222.

[59] J. Brooks, K. Gould, J. Smith, Isoprenoid hydrocarbons in coal and petroleum, Nature 222 (5190) (1969) 257–259.

[60] M. Farhaduzzaman, W.H. Abdullah, M.A. Islam, M. Pearson, Source rock potential of organic-rich shales in the Tertiary Bhuban and Boka bil Formations, Bengal basin, Bangladesh, J. Petrol. Geol. 35 (4) (2012) 357–375.

[61] D. Large, A. Gize, Pristane/phytane ratios in the mineralized Kupferschiefer of the Fore-Sudetic Monocline, southwest Poland, Ore Geol. Rev. 11 (1-3) (1996) 89–103.

[62] H. Ten Haven, J. De Leeuw, J.S. Damsté, P. Schenck, S. Palmer, J. Zumberge, Application of biological markers in the recognition of palaeohypersaline environments, Geol. Soc. Lond. Spec. Publ. 40 (1) (1988) 123–130.

[63] T. Vu, K.-G. Zink, K. Mangelsdorf, R. Sykes, H. Wilkes, B. Horsfield, Changes in bulk properties and molecular compositions within New Zealand Coal Band solvent extracts from early diagenetic to catagenetic maturity levels, Org. Geochem. 40 (9) (2009) 963–977.

[64] J. Van Koeverden, D. Karlsen, K. Backer-Owe, Carboniferous non-marine source rocks from spitsbergen and bjørnøya: comparison with the western arctic, J. Petrol. Geol. 34 (1) (2011) 53–66.

[65] P.A. Meyers, L.R. Snowdon, Types and Thermal Maturity of Organic Matter Accumulated during Early Cretaceous Subsidence of the Exmouth Plateau, Northwest Australian Margin: Chapter 8, 1993.

[66] W.S. El Diasty, J. Moldowan, Application of biological markers in the recognition of the geochemical characteristics of some crude oils from Abu Gharadig Basin, north Western Desert–Egypt, Mar. Petrol. Geol. 35 (1) (2012) 28–40.

[67] D.W. Waples, Biomarkers for geologists-a practical guide to the application of steranes and triterpanes in petroleum geology, Chap 2 (1991) 5–10.

[68] W.H. Abdullah, Organic facies variations in the Triassic shallow marine and deep marine shales of central Spitsbergen, Svalbard, Mar. Petrol. Geol. 16 (5) (1999) 467–481.

[69] G. Ourisson, P. Albrecht, M. Rohmer, The hopanoids. Palaeochemistry and biochemistry of a group of natural products, Pure Appl. Chem. 51 (4) (1979) 709–729.

[70] K. Gürgey, Geochemical characteristics and thermal maturity of oils from the Thrace Basin (western Turkey) and western Turkmenistan, J. Petrol. Geol. 22 (2) (1999) 167–189.

[71] J.S.S. Damsté, et al., Evidence for gammacerane as an indicator of water column stratification, Geochimica et Cosmochimica Acta 59 (9) (1995) 1895–1900.

[72] L. Marynowski, M. Narkiewicz, C. Grelowski, Biomarkers as environmental indicators in a carbonate complex, example from the Middle to upper devonian, holy cross mountains, Poland, Sediment. Geol. 137 (3-4) (2000) 187–212.

[73] F.d. Aquino Neto, Occurrence and formation of tricyclic and tetracyclic terpanes in sediments and petroleum, Adv. Org. Geochem. 1981 (1983) 659–667.

[74] J. Volkman, M. Banks, K. Denwer, F. Aquino Neto, Biomarker composition and depositional setting of Tasmanite oil shale from northern Tasmania, Australia, in: 14th International Meeting on Organic Geochemistry, 1989, pp. 18–22.

[75] R.t. Philp, T. Gilbert, Biomarker distributions in Australian oils predominantly derived from terrigenous source material, Org. Geochem. 10 (1-3) (1986) 73–84.

[76] H. Volk, S.C. George, H. Middleton, S. Schofield, Geochemical comparison of fluid inclusion and present-day oil accumulations in the Papuan Foreland–evidence for previously unrecognised petroleum source rocks, Org. Geochem. 36 (1) (2005) 29–51.

[77] K.E. Peters, C.C. Walters, J.M. Moldowan, The Biomarker Guide: II. Biomarkers and Isotopes in Petroleum Systems and Earth History, Cambridge University Press, 2004.

[78] J.K. Volkman, A review of sterol markers for marine and terrigenous organic matter, Org. Geochem. 9 (2) (1986) 83–99.

[79] W.-Y. Huang, W. Meinschein, Sterols as ecological indicators, Geochimica et cosmochimica acta 43 (5) (1979) 739–745.

[80] P.D. Nichols, A.C. Palmisano, M.S. Rayner, G.A. Smith, D.C. White, Occurrence of novel C30 sterols in Antarctic sea-ice diatom communities during a spring bloom, Org. Geochem. 15 (5) (1990) 503–508.

[81] H.Z. Hossain, Y. Sampei, B.P. Roser, Characterization of organic matter and depositional environment of Tertiary mudstones from the Sylhet Basin, Bangladesh, Org. Geochem. 40 (7) (2009) 743–754.

[82] E. Bray, E. Evans, Distribution of n-paraffins as a clue to recognition of source beds, Geochimica et Cosmochimica Acta 22 (1) (1961) 2–15.

[83] A. Mackenzie, R. Patience, J. Maxwell, M. Vandenbroucke, B. Durand, Molecular parameters of maturation in the Toarcian shales, Paris Basin, France—I. Changes in the configurations of acyclic isoprenoid alkanes, steranes and triterpanes, Geochimica et Cosmochimica Acta 44 (11) (1980) 1709–1721.

[84] W.K. Seifert, J.M. Moldowan, Applications of steranes, terpanes and monoaromatics to the maturation, migration and source of crude oils, Geochimica et Cosmochimica Acta 42 (1) (1978) 77–95.

[85] W.K. Seifert, J.M. Moldowan, Paleoreconstruction by Biological Markers, 1980.

[86] E. Gallegos, J. Moldowan, The effect of injection hold time on GC resolution and the effect of collision gas on mass spectra in geochemical biomarker] 2 research, Preprint Am. Chem. Soc. Div. Petrol. Chem. 34 (1) (1989) 159–169.

[87] J. Rullkötter, R. Marzi, Natural and artificial maturation of biological markers in a Toarcian shale from northern Germany, Org. Geochem. 13 (4-6) (1988) 639–645.

[88] S. Korkmaz, R.K. Gülbay, Organic geochemical characteristics and depositional environments of the Jurassic coals in the eastern Taurus of Southern Turkey, Int. J. Coal Geol. 70 (4) (2007) 292–304.